

Neural Correlates of Smooth Pursuit Eye Movements in Schizotypy and Recent Onset Psychosis: A Multivariate Pattern Classification Approach

Rebekka Schröder¹, Eliana Faiola¹, Maria Fernanda Urquijo², Katharina Bey³, Inga Meyhöfer¹, Maria Steffens¹, Anna-Maria Kasparbauer¹, Anne Ruef², Hanna Högenauer³, René Hurlemann^{4,5}, Joseph Kambeitz^{6,*}, Alexandra Philipsen³, Michael Wagner³, Nikolaos Koutsouleris², and Ulrich Ettinger^{1,*}

¹Department of Psychology, University of Bonn, Kaiser-Karl-Ring 9, 53111, Bonn, Germany; ²Department of Psychiatry and Psychotherapy, Ludwig-Maximilians-University of Munich, Nußbaumstr. 7, 80336, Munich, Germany; ³Department of Psychiatry and Psychotherapy, University of Bonn, Sigmund-Freud-Str. 25, 53127, Bonn, Germany; ⁴Department of Psychiatry, University of Oldenburg Medical Campus, Hermann-Ehlers-Str. 7, 26160, Bad Zwischenahn, Germany; ⁵Department of Psychiatry and Division of Medical Psychology, University Hospital Bonn, Venusberg-Campus 1, 53127, Bonn, Germany; ⁶Department of Psychiatry and Psychotherapy, University of Cologne, Faculty of Medicine and University Hospital Cologne, Kerpener Str. 62, 50931, Cologne, Germany

*To whom correspondence should be addressed: Department of Psychology, University of Bonn, Kaiser-Karl-Ring 9, 53111 Bonn, Germany, tel: +49 228 734208, fax: +49 228 7362323, e-mail: ulrich.ettinger@uni-bonn.de

Schizotypy refers to a set of personality traits that bear resemblance, at subclinical level, to psychosis. Despite evidence of similarity at multiple levels of analysis, direct comparisons of schizotypy and clinical psychotic disorders are rare. Therefore, we used functional magnetic resonance imaging (fMRI) to examine the neural correlates and task-based functional connectivity (psychophysiological interactions; PPI) of smooth pursuit eye movements (SPEM) in patients with recent onset psychosis (ROP; $n = 34$), participants with high levels of negative (HNS; $n = 46$) or positive (HPS; $n = 41$) schizotypal traits, and low-schizotypy control participants (LS; $n = 61$) using machine-learning. Despite strong previous evidence that SPEM is a highly reliable marker of psychosis, patients and controls could not be significantly distinguished based on SPEM performance or blood oxygen level dependent (BOLD) signal during SPEM. Classification was, however, significant for the right frontal eye field (FEF) seed region in the PPI analyses but not for seed regions in other key areas of the SPEM network. Applying the right FEF classifier to the schizotypal samples yielded decision scores between the LS and ROP groups, suggesting similarities and dissimilarities of the HNS and HPS samples with the LS and ROP groups. The very small difference between groups is inconsistent with previous studies that showed significant differences between patients with ROP and controls in both SPEM performance and underlying neural mechanisms with large effect sizes. As the current study had sufficient power to detect such differences, other reasons are discussed.

Key words: machine-learning, schizophrenia spectrum, eye movements, functional magnetic resonance imaging

Introduction

Schizotypy refers to a set of personality traits that resemble the symptoms of psychosis in an attenuated, subclinical form.¹ Similarities of schizotypy with psychosis include cognitive deficits, morphological and functional neural correlates and environmental risk factors.^{1–5} Despite these similarities,^{1–14} transition rates from schizotypy to psychosis are low.^{15,16} This may suggest that although persons with high schizotypy carry risk for psychosis, protective mechanisms operate which lower the risk of transition.^{17–19} Alternatively, high schizotypy may result from insufficiency of risk factors for psychosis (despite higher risk than in low-schizotypy).^{16,20} These theoretical issues aside, there should not only be similarities, but also dissimilarities between schizotypy and psychotic disorders. Several such differences have been reported. Contradictory to findings of volume reductions in schizophrenia,^{10,21–25} schizotypy is associated with increased cortical thickness in frontal lobe¹² and volume in cingulate cortex.^{26,27} Additionally, positive schizotypy is also associated with beneficial characteristics, such as enhanced creativity.^{28,29}

However, studies directly comparing people with high levels of schizotypy and patients with psychotic disorders are scant,³⁰ although this is essential to detect

both similarities and differences.^{3,19} The present study, therefore, compared positive and negative schizotypal individuals to patients with recent onset psychosis and low-schizotypy controls in one of the most robust biomarkers of psychosis, smooth pursuit eye movements (SPEM).^{31–33} Whilst persons with high schizotypy have been reported to show impaired SPEM,^{34–40} differences to psychotic patients have also been detected in indirect comparisons. For example, the neural correlates of SPEM in schizotypy and schizophrenia show only partial overlap. Whilst both persons with high schizotypy and patients exhibit reduced activity in visual areas (e.g., occipital cortex),^{36,41–44} reductions in frontal areas (e.g., frontal eye fields) found in schizophrenia^{41,42,44} have not been observed in schizotypy.³⁶ However, no direct comparison between schizotypal individuals and schizophrenia patients is available.

Importantly, previous studies have found not only altered brain structure and function in schizophrenia,^{10,21–25,41–44} but also aberrant brain connectivity,^{45–48} a finding that has also been demonstrated in persons with high schizotypy.^{49–55} However, it has not previously been investigated whether functional connectivity during SPEM is altered in schizophrenia or schizotypy.

A final issue addressed here is that previous fMRI studies of SPEM have relied on univariate analyses.^{36,41–44} However, classical fMRI analyses involve between-group overlap (i.e., despite brain activation differences between two groups, they show substantial overlap at certain voxels, reducing the likelihood of detecting the differences^{56,57}), a problem addressed by multivariate machine-learning analyses^{57,58}: instead of focusing on between-group differences regarding certain voxels, machine-learning allows to predict whether a participant belongs to group A (e.g., controls) or group B (e.g., patients) based on activity or connectivity patterns.^{57,59} Moreover, the likelihood of a third group (e.g., persons with high schizotypy) being identified as controls or patients can be examined. Machine-learning has been shown to separate patients with a psychotic disorder and controls with high accuracy^{58,60–63} and is sensitive to effects of schizotypy.^{64,65}

We hypothesized that patients and controls would be differentiated with significant accuracy.^{31,58,60–62} The strongest contribution to this differentiation was expected from brain regions known to underlie SPEM⁶⁶ or its dysfunction in schizophrenia.^{43,44,67} Additionally, we explored whether persons with high schizotypy would be classified more as controls or as patients. We distinguished between persons with high schizotypy with primarily positive or negative schizotypal traits to explore potential differences regarding the classification. As SPEM deficits in schizotypy are less pronounced than in schizophrenia,^{35,39,40} and activity reductions during SPEM in schizotypy show only partial overlap with those in schizophrenia,³⁶ persons with high schizotypy might be classified between patients and controls. Certain brain regions (e.g., occipital cortex³⁶)

might contribute to proximity of persons with high schizotypy and patients with ROP, while other areas (e.g., frontal eye fields³⁶) might lead to higher classification of persons scoring high on schizotypy to the control group.

Methods

Recruitment and Selection of Participants

Participants for both schizotypy groups and the low-schizotypy control group were recruited from the general population through an online version of the Oxford-Liverpool Inventory of Feelings and Experiences short (O-LIFE, German version⁶⁸), advertised via flyers and social media. Cut-offs for group assignment were based on an O-LIFE database of $n = 5006$ ¹. Assignment to the positive schizotypy group (HPS) required a score ≥ 1.25 SD above the same sex mean on the unusual experiences (UE) and ≤ 0.5 SD below the same sex mean on the Introverted Anhedonia (IA) scale, and vice versa for the negative schizotypy group (HNS), as described previously.⁴⁰ Participants were assigned to the low-schizotypy control group (LS) if they scored ≤ 0.5 SD below the same sex mean on both UE and IA scales. Participants who met these criteria were invited to a telephone screening in order to discuss exclusion criteria (see below for details).

Patients with recent onset psychosis (ROP) were recruited from in-patient and out-patient services. They were included in the study if they had i) a diagnosis of a psychotic disorder according to DSM-IV or ICD-10 criteria (F20, F22, F23, F25, F29) for a maximum of three years, with no more than one psychotic episode in the past, as determined by a medical doctor, and ii) a score of 6 on at least one of the P1–P5 items of the Structural Interview of Prodromal Symptoms (SIPS⁶⁹). Moreover, patients were screened for exclusion criteria listed below.

The study was approved by the ethics committees of the Faculty of Medicine, University of Bonn, and the Faculty of Medicine, University of Munich. Participants provided written informed consent and were financially rewarded.

Exclusion criteria for all participants were age < 18 and > 40 , insufficient knowledge of German, any neurological disorder, visual impairments (except for glasses/lenses) or eye surgery, MRI exclusion criteria such as pregnancy, claustrophobia and the presence of metal in the body, traumatic brain injury with loss of consciousness for more than five minutes, systemic disease involving the central nervous system, and a positive result in an alcohol (ACE AL5500) or drug screening (Drug-Screen Multi 5T, nal von minden GmbH) during the time of the assessment.

Additional exclusion criteria for the schizotypy and control groups were having a first-degree relative with a psychotic disorder, regular medication intake except for contraceptives or thyroid medication, and any

¹<https://osf.io/bfxmt/>

present Axis I disorder or past or present psychotic disorder (MINI International Neuropsychiatric Interview German Version 5.0.0⁷⁰). In addition, participants with clinical high-risk for psychosis criteria according to the SIPS⁶⁹ were excluded. Additional exclusion criteria for patients were acute or chronic organic brain syndromes such as dementia or delirium, bipolar disorder, and unipolar depression with psychotic symptoms.

Study Procedure

Schizotypal and control participants first completed the O-LIFE and were then contacted via telephone for an informal briefing on the study, and then screened via telephone or in a personal meeting. For all groups, this initial screening was followed by two study sessions at intervals of no more than 1 month.

Participants were instructed not to drink alcohol starting one day before the study session, not to consume any caffeine 2 h before the session, and to get normal sleep the night before the session. The first study session included i) a screening for current alcohol and drug consumption, ii) SIPS and the Schizophrenia Proneness Instrument, Adult Version (SPI-A⁷¹), iii) a neuropsychological test battery, and iv) the *vocabulary* and *matrices* subtests of the WAIS-III as a measure of intelligence.⁷² The second study session included i) a screening for current alcohol and drug consumption, and ii) an MRI measurement including a structural scan and two fMRI scans with concurrent oculographic measurement of SPEM and antisaccades. In addition, participants filled out several questionnaires as an online version from home.

SPEM Task. The SPEM task was programmed in ExperimentBuilder (SR Research Ltd., Ontario, Canada). Participants viewed a 32-inch MRI-compatible TFT LCD monitor (NordicNeuroLab, Bergen, Norway; resolution: 1024 × 768 pixels, refresh rate: 120 Hz) via a first-surface reflection mirror mounted on the head coil. They were instructed to follow a target with their eyes (SPEM blocks) and to fixate the target (fixation blocks) as accurately as possible whilst keeping the head still. The distance from participants' eyes to screen was 1600 mm. The target was a gray (RGB = 128,128,128) circle (diameter = 0.36°, stroke width = 0.11°) moving horizontally across the screen in front of a black (RGB = 0,0,0) background (figure 1). It moved horizontally in a sinusoidal pattern at low (0.2 Hz) and high velocity (0.4 Hz), and an excursion of $\pm 5.7^\circ$ from the center. SPEM blocks (duration: 30 s each) alternated with fixation blocks (duration: 20 s each). During fixation blocks, the target was stationary in the center of the screen. In total, ten SPEM blocks (five each with low and high target frequencies) and ten fixation blocks were presented. A horizontal three-point calibration was carried out before the task. Movements of the right eye were recorded with an

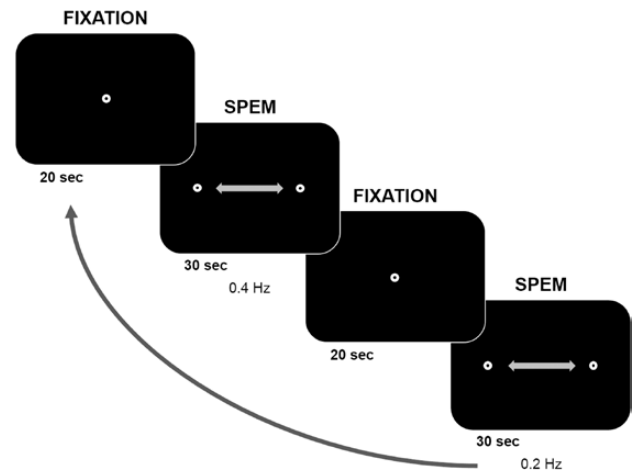


Fig. 1. Graphic representation of the fMRI SPEM task. 10 blocks of fixation (duration: 20 s each) alternate with 10 blocks of sinusoidal SPEM (5 blocks with a target velocity of 0.4 Hz, 5 blocks with a target velocity of 0.2 Hz; duration: 30 s each). During SPEM blocks, the target moves with an excursion of $\pm 5.7^\circ$ from the center.

MRI-compatible video-based eye-tracker (EyeLink 1000, SR Research Ltd., Ontario, Canada; sampling rate 1000 Hz).

fMRI Data Acquisition. A Siemens 3 T Trio Scanner (Bonn) and a Philips Ingenia 3 T Scanner (Munich) were used. To reduce noise from the scanner, participants wore earplugs, and foam pads helped to minimize head movements. For radio frequency transmission and reception, both sites used a 32-channel head coil. First, a localizer scan was acquired to place the volume of interest. Then, a high-resolution structural scan for image co-registration and normalization was acquired, using the following parameters in Bonn (and in Munich): TR = 1600 ms, TE = 2.54 ms (5.53 ms), inversion time = 850 ms, flip angle = 9° (8°), FoV = 256 mm, matrix size = 320 × 320 (256 × 256), 160 slices (190 slices), slice thickness = 0.8 mm (1.0 mm), sequential slice-order with no inter-slice gap, and voxel size = 0.8 × 0.8 × 0.8 (0.9 × 0.9 × 0.9). During the SPEM task, at both sites, T2*-weighted MRI scans were collected with gradient-echo planar imaging sequences (TR = 2500 ms, TE = 30 ms, flip angle = 90°) that displayed the blood oxygenation level dependent (BOLD) response. Additional scan parameters were as follows: FoV = 192 mm; matrix size = 96 × 96; 37 slices; slice thickness = 3 mm; sequential slice-order with inter-slice gap of 0.3 mm; voxel size = 3 × 3 × 3. Slices were oriented parallel to the intercommissural plane (AC-PC line). 208 whole brain images were collected for each participant.

Data Processing

Behavioral Data. Data quality was first examined with DataViewer (SR Research Ltd., Ontario, Canada), before

being processed using scripts (See footnote 1) in Matlab (The Mathworks, Natick, MA), calculating SPEM parameters from eye position coordinates and time stamps in the raw data. Dependent variables were velocity gain (mean eye velocity relative to mean target velocity in %), root mean square error (RMSE, in degrees) and saccade frequency (N/s). SPEM variables were calculated for each of the frequencies (0.2 and 0.4 Hz) separately, excluding the first half-cycle of each block. Velocity gain was calculated for segments of pursuit in the middle 50% of each half-cycle, excluding blinks and saccades.³⁸ Saccadic frequency was calculated using amplitude ($\geq 1^\circ$), acceleration ($\geq 3800^\circ/s^2$) and velocity ($\geq 30^\circ/s$) criteria. RMSE scores were calculated excluding blinks. A blink was identified automatically when the eye-tracker did not detect any eye position. Saccades occurring immediately before or after a blink were excluded for all SPEM parameter calculations.

fMRI Data. Data preprocessing and first-level analysis were performed using Statistical Parametric Mapping 12 (SPM12; <https://www.fil.ion.ucl.ac.uk/spm/software/>) running in MATLAB R2017a (The MathWorks, Natick, MA).

Data preprocessing included realignment of the images of each participant along the mean image in the time series to correct for head motion, using a least squares approach and a six-parameter rigid-body transformation. Additionally, images were unwarped to correct for image distortions due to magnetic field inhomogeneities. Second, functional scans were co-registered to the T1-weighted anatomical image. Then, structural images were segmented in order to separate grey matter, white matter and cerebro-spinal fluid. The segmented images were used for normalization, in order to transform all images into standard space (Montreal Neurological Institute, MNI template) using 12-parameter affine linear transformation. Smoothing was applied using a Gaussian full-width-at-half-maximum filter of 8 mm.

First-level analyses were conducted to create, for each participant, a contrast for i) SPEM vs. Fixation blocks and ii) High Velocity vs. Low Velocity blocks (not thresholded). These contrasts were then used for pattern classification (see below). For first-level analysis, a general linear model was used, including a SPEM vector (all SPEM blocks) and a Velocity vector (0.2 Hz, 0.4 Hz). These vectors were contrasted against fixation. Six motion parameters entered the analysis as additional regressors. BOLD response was modelled as a canonical hemodynamic response-function. At the second level, each contrast was compared between-groups using one-way ANCOVA with site (Bonn, Munich) and sex (male, female) as covariates.

In addition, generalized psychophysiological interaction analyses^{73,74} (gPPI) were performed to explore group differences in task-based functional connectivity of the pursuit network. Key areas of the pursuit network (LGN,

V1, V5, posterior parietal cortex [PPC], frontal eye fields [FEF]) were selected as seed regions and seed coordinates were taken from a previous publication⁷⁵ (Supplementary table 1). To accommodate individual differences in the location of task activations and thus define individual seed spheres, first, for each region a 12 mm sphere was positioned around the coordinates derived from previous literature. Second, the largest individual task activation peak (omnibus-F-map, corrected at $P < .001$) within this sphere was identified and a smaller (4 mm sphere) was centered around these peak coordinates. For those participants, for whom no peak could be identified in the larger sphere, the 4 mm-sphere was centered around the literature-derived coordinates.

To determine the gPPI regressors, the first eigenvariate of the timeseries of all voxels within each individual sphere was extracted, deconvolved, multiplied with the task regressors and reconvolved with the HRF. Then, for each seed region, a GLM model was set up which included the psychophysiological interaction terms and the task and seed region timeseries vectors as regressors as well as the six motion vectors from the realignment preprocessing step as covariates of no interest. Two first-level contrasts were determined (PPI SPEM vs. fixation, PPI high velocity vs. low velocity SPEM) for each participant and each seed region, resulting in a total of 20 models per participant. These contrasts were taken to the second level for one-way ANCOVAs to analyze between-group differences with site and sex defined as covariates.

All fMRI results were family-wise error corrected (FWE, $P < .05$). Anatomical labels were obtained using the Anatomy Toolbox.⁷⁶

Pattern Classification

Behavioral Data. To generate a classification model distinguishing between LS and ROP based on behavioral SPEM data, we established a machine-learning pipeline using NeuroMiner (<http://www.proniapredictors.eu/neurominer/index.html>). As behavioral data we used gain, saccade frequency and RMSE at each target velocity.

To first train the classification models and then evaluate their accuracy, we conducted a repeated nested cross-validation (CV^{77,78}), with an inner CV cycle (CV1) to train and select optimally discriminative models, and an outer CV cycle (CV2) to validate the best models from CV1. Preprocessing of CV1 data included correction for effects of site and sex. To ensure that we corrected only for effects that were not attributable to disease-related factors, we added the variables as covariates and calculated beta coefficients only for the LS group, using partial correlation analysis. Then, we residualized the patient and healthy control data using the calculated coefficients.^{78,79} Finally, data were scaled to [0, 1].

For both inner (CV1) and outer (CV2) cycles, we chose a 10 (folds/partitions) \times 10 (permutations) CV, with each

permutation performing a reshuffling of participants within their groups. While in CV2, one partition at a time was held back as validation data, the nine remaining partitions entered CV1 as training data. In CV1, to create the classification models, 10 partitions with 10 repetitions were used. This means that for each validation fold at CV2, 100 different training data partitions were generated at CV1. In each training partition, linear support vector machines (LIBSVM 3.12; <http://www.csie.ntu.edu.tw/~cjlin/libsvm>) were used to find the hyperplane that separates best between the groups. This is done by maximizing the margin between the nearest data points of opposite classes.⁵⁸ Penalty strength was optimized as a hyperparameter with a range from 0.015624 to 16 in 11 steps. In addition, we weighted the hyperplane due to unequal sample sizes in the LS and ROP groups. This procedure yielded decision scores measuring the likeliness of a given participant being in the control or the patient group. The most discriminative sets of features were determined in each of these 100 training partitions. Each of the trained classification models was used to predict the group membership of the validation fold in CV2. Support vector machine-learning has been intensively applied in the study of psychosis during the last years and has, therefore, become one of the most established methods in this field.^{58,60,63,78,80,81} Therefore, and to facilitate comparability with previous studies, we applied this method in the present study.

To measure the classifier's performance, we used sensitivity, specificity, and balanced accuracy [(sensitivity + specificity)/2]. To calculate the significance of the classification, we conducted a permutation analysis with 1000 random class label permutations. The null hypothesis, stating that the classifier cannot predict group memberships correctly, was rejected at $\alpha = .05$.

fMRI Data. To distinguish LS from ROP based on neural correlates of SPEM, we used first-level contrast images (SPEM vs. Fixation; high vs. low target velocity; 10 gPPI SPEM vs. Fixation contrasts and 10 gPPI high vs. low target velocity for each seed region in the left and right hemisphere) for the machine-learning pipeline.

The preprocessing of the BOLD data was identical to the behavioral data analysis, except for three additional steps: First, we pruned the data, in order to prevent overfitting of the algorithm. More precisely, we removed features with no variance within a fold as well as features with infinity values. Second, to correct for effects of site, we applied ComBat batch effect correction. Next, we applied principal component analysis (PCA) by mapping correlated voxels to a number of uncorrelated principal components. PCA was used as a statistical smoothing technique to reduce the dimensionality of discriminative patterns and eliminate noise.^{58,78} The number of PCA components was optimized within the nested cross-validation approach described above. Specifically, the

number of components was determined by the optimal PCA energy for class separation ranging from 0.5 to 0.9. Finally, data were scaled voxel-wise to [0, 1] following again a strict separation of CV1 training, CV1 test and CV2 validation data, where the scaling parameters were derived from the CV1 training sample and then applied to other data partitions.

The training pipeline for the BOLD data was identical to the pipeline for the behavioral data.

For reasons of computational efficiency, the permutation analyses for calculating the significance of the classification algorithms for the connectivity maps were first applied only to the first CV2 fold. If a classification algorithm was significant at trend-level ($P < .10$) in this fold, the permutation analyses were repeated for all 10 CV2 folds to ensure robustness of the results. Resulting P -values were corrected for multiple testing separately for each contrast (SPEM and Velocity) using the false discovery rate procedure.⁸²

Sign-based consistency mapping was applied to determine brain areas contributing to classification of LS and ROP.⁸³ Images were thresholded at $-\log_{10}(0.05)$, FDR-corrected.

In addition, stacking analyses were performed separately for the SPEM and Velocity contrasts in order to combine the predictions of the lower order classification algorithms. To do so, the decision scores from all modalities of each contrast (i.e., the standard fMRI contrast and all 10 gPPI contrasts) were entered into a single analysis, yielding two stacked analyses (SPEM contrast, Velocity contrast). The training pipeline of these stacked data sets was identical to the pipeline of the lower order fMRI trainings. The stacking pipeline was wrapped into the same repeated nested cross-validation setup as described above to exclude the possibility of information leakage, i.e., the first-level decision scores of a given CV1 partition were forwarded to the second-level SVM, which was then applied to the second-level CV2 data alongside the other trained SVM models of the given CV2 partition.

Model Application to Schizotypal Samples. In case of a significant classification, the trained models used to predict group membership for LS and ROP were applied to persons with high schizotypy. This allows to examine whether a schizotypal participant is more likely to be classified as LS or ROP, and thus, whether BOLD data during SPEM in schizotypy are more similar to those of LS or ROP. It produces decision scores indicating whether a participant is more likely to belong to the LS (positive decision scores) or the ROP group (negative scores). One-way ANOVA was employed to indicate whether the decision scores differed between groups.

In addition, a regression analysis was conducted where the HPS and HNS decision scores were used as a regressor to predict BOLD activity in the HPS and HNS groups.

Univariate Group Comparisons for Behavioral SPEM Data

In addition to the classification analysis, we conducted mixed ANCOVA based on the behavioral SPEM data, with *Group* as a between- and *Velocity* as a within-subjects factor. Three separate analyses were conducted, with gain, saccade frequency or RMSE as dependent variables, and site (Bonn, Munich) and sex (male, female) as covariates.

Results

Descriptive Statistics, Sociodemographic and Clinical Variables

No significant group differences were found with respect to age and years of formal education. However, there were differences in distributions of participants across sites, as well as in sex distributions and intelligence (table 1). For additional characteristics of the ROP sample see table 2. Descriptive statistics of SPEM parameters are in table 3.

Behavioral Results

A total of 174 participants were included for the behavioral analyses (see table 3 for the number of participants in each group). Nine participants had to be excluded due to poor eye-tracking quality.

Classification Analysis. Based on behavioral data, LS and ROP participants were classified with a balanced accuracy of 52.1% (sensitivity = 71.9%; specificity = 32.4%), which was not significant ($P = .438$, AUC = 0.56).

Univariate Group Comparisons. Mixed ANCOVA with all four groups revealed main effects of Velocity for all three parameters (gain: $F_{(1,168)} = 54.02, P < .001, \eta_p^2 = .24$; RMSE: $F_{(1,168)} = 61.46, P < .001, \eta_p^2 = .27$; saccade frequency: $F_{(1,168)} = 40.89, P < .001, \eta_p^2 = .20$). Additionally, there was a main effect of Group on RMSE ($F_{(3,168)} = 2.92, P = .036, \eta_p^2 = .05$). Post-hoc pair-wise comparisons showed significant differences between the LS and ROP group that did not, however, survive Bonferroni-correction (table 4). For saccade frequency and gain, there were no significant effects of Group, although there was a trend towards a main effect of Group on gain ($P = .079$). There were no Group by Velocity interactions (all $P > .126$). Statistical parameters and effect sizes of all pairwise group comparisons are in table 4.

fMRI Results

A total of 180 participants were included for the fMRI analyses. Three participants (2 LS, 1 ROP) had to be excluded due to poor fMRI data quality.

BOLD Task and Group Effects. There were no significant group differences for the SPEM or Velocity contrasts. However, the smooth pursuit task (SPEM contrast) activated areas of the pursuit network (figure 2 and Supplementary tables 2 and 3 for results in the LS group). The Velocity contrast revealed significant activations in visual cortex (figure 2 and Supplementary table 4 for results in the LS group). There were no significant differences for the reverse Velocity contrast.

Table 1. Sociodemographic and clinical variables of the four study groups

Variable	LS (n = 62)	HPS (n = 41)	HNS (n = 46)	ROP (n = 34)	Statistics
Site (n Bonn/Munich)	31/31	28/13	29/17	12/22	$\chi^2_{(3)} = 10.07, P = .02$
Sex (n female/male)	29/33	26/15	25/21	10/24	$\chi^2_{(3)} = 9.28, P = .03$
Age (in years; M, SD)	25.94 (4.73)	26.24 (6.33)	26.67 (4.61)	25.09 (4.98)	$F_{(3,179)} = 0.65, P = .58, \eta_p^2 = 0.01$
O-LIFE scores (M, SD)					
UE	1.21 (1.19)	9.46 (1.80)	1.48 (1.19)	N/A	$F_{(2,146)} = 513.89, P < .001, \eta_p^2 = 0.88$
IA	1.03 (0.75)	1.27 (0.81)	6.33 (1.01)	N/A	$F_{(2,146)} = 592.55, P < .001, \eta_p^2 = 0.89$
CD	3.17 (2.52)	5.97 (2.98)	6.00 (2.93)	N/A	$F_{(2,146)} = 17.27, P < .001, \eta_p^2 = 0.21$
Total	5.34 (3.46)	16.62 (4.45)	13.67 (3.62)	N/A	$F_{(2,146)} = 114.49, P < .001, \eta_p^2 = 0.63$
Years of formal education (M, SD)	16.83 (3.26)	16.32 (3.15)	16.72 (3.45)	15.20 (3.50)	$F_{(3,173)} = 1.91, P = .13, \eta_p^2 = 0.03$
Verbal intelligence test score ^a (M, SD)	12.02 (2.98)	10.98 (2.62)	11.59 (2.61)	9.47 (3.33)	$F_{(3,177)} = 5.87, P = .001, \eta_p^2 = 0.09$
Nonverbal intelligence test score ^b (M, SD)	11.21 (1.91)	11.24 (1.95)	11.22 (1.82)	9.42 (3.56)	$F_{(3,178)} = 5.57, P = .001, \eta_p^2 = 0.09$

Notes: LS, low-schizotypy; HPS, high positive schizotypy; HNS, high negative schizotypy; ROP, recent onset psychosis; O-LIFE, Oxford-Liverpool Inventory of Feelings and Experiences; UE, unusual experiences; IA, introverted anhedonia; CD, cognitive disorganization; N/A, not available.

^aWechsler Adult Intelligence Scale (WAIS) vocabulary subtest.

^bWAIS matrices subtest.

Connectivity Analysis. gPPI analyses yielded no significant differences between the four groups for any of the seed regions or contrasts. However, wide-spread connectivity maps for the SPEM contrast for all seed regions could be observed (Supplementary figures 1 and 2 and tables 5–14 for results in the LS group). There were no significant connectivity maps for the Velocity contrasts.

Classification Analysis. Based on the SPEM contrast, LS and ROP participants were separated with a balanced accuracy of 55.6% (sensitivity = 56.7%, specificity = 54.5%) which was not significant ($P = .297$, AUC = 0.63). Based on the Velocity contrast, classification reached a balanced accuracy of 44.5% (sensitivity = 61.7%; specificity = 27.3%), which was also not significant ($P = .392$, AUC = 0.47).

Classification results of the gPPI analyses were significant for the SPEM contrast in right FEF (table 5). For this seed region, LS and ROP participants were separated

Table 2. Clinical characteristics of the ROP group

Variable	ROP ($n = 34$)
Time since illness onset (in days; M , SD)	281.40 (302.45)
Diagnosis (n)	
Schizophrenia	22
Delusional disorder	2
Brief psychotic disorder	5
Schizoaffective disorder	4
Unspecified nonorganic psychosis	1
PANSS scores (M , SD)	
Positive	20.64 (5.52)
Negative	16.84 (8.37)
General psychopathology	36.96 (16.29)
Medication (n)	
Typical	–
Atypical	19
Both	5
No medication	4
Unknown	6

Notes: ROP, recent onset psychosis; PANSS, Positive and Negative Symptom Scale.

Table 3. Descriptive statistics for SPEM parameters

Target velocity	Variable	LS ($n = 57$)	HPS ($n = 41$)	HNS ($n = 42$)	ROP ($n = 34$)
0.2 Hz	Gain (%)	91.19 (9.59)	90.73 (11.70)	90.36 (11.49)	86.89 (14.50)
	RMSE (°)	1.45 (0.75)	1.45 (0.54)	1.46 (0.64)	1.93 (1.09)
	Frequency of saccades (N/s)	0.67 (0.38)	0.66 (0.38)	0.75 (0.45)	0.82 (0.45)
0.4 Hz	Gain (%)	75.95 (11.99)	71.77 (15.28)	71.89 (17.00)	68.53 (18.27)
	RMSE (°)	1.99 (0.76)	2.15 (0.67)	2.09 (0.81)	2.23 (0.93)
	Frequency of saccades (N/s)	1.47 (0.44)	1.50 (0.46)	1.56 (0.51)	1.60 (0.49)

Notes: Data represent means (standard deviations). LS, low-schizotypy; HPS, high positive schizotypy; HNS, high negative schizotypy; ROP, recent onset psychosis; RMSE, root mean square error.

with a balanced accuracy of 62.4% (sensitivity = 73.3%; specificity = 51.5%) which was significant ($P = .009$; AUC = 0.63) before but not after correcting for multiple testing (FDR; $P = .090$).

Visualization of the machine-learning results revealed that classification was based on connectivity from right FEF to parahippocampal gyrus and hippocampus, striatum, thalamus, cerebellum, anterior and posterior cingulate gyrus, postcentral gyrus, superior parietal cortex, lateral occipital cortex and fusiform gyrus, supramarginal and angular gyrus, precuneus, temporal pole, inferior temporal gyrus, frontal pole and frontal-medial cortex (Supplementary figure 3).

Stacking Analyses. In the stacking analyses of the SPEM contrast, LS and ROP participants were separated with a balanced accuracy of 55.4% (sensitivity = 68.3%, specificity = 42.4%) which was not significant ($P = .748$, AUC = 0.56). Based on the Velocity contrast, classification reached a balanced accuracy of 43.3% (sensitivity = 53.3%; specificity = 33.3%), which was not significant ($P = .941$, AUC = 0.35).

Model Application to Schizotypal Samples. The classification model of the right FEF SPEM gPPI contrast was significant before correction for multiple testing. Therefore, in an explorative analysis, we applied the classification algorithm to the schizotypal samples to determine whether persons with high schizotypy would be classified as LS or ROP. Sixteen HPS and 18 HNS were classified as ROP, and 25 HPS and 28 HNS were classified as LS. Descriptively, decision scores of persons with high schizotypy were in between LS and ROP (Supplementary table 15). However, one-way ANOVA for comparison of decision scores between groups was not significant ($F_{(3,179)} = 1.51$, $P = .214$, $\eta_p^2 = 0.025$).

In an additional regression analysis in both schizotypal samples, lower decision scores were associated with increased gPPI connectivity from right FEF to clusters in angular gyrus, precuneus, hippocampus and parahippocampus, postcentral and precentral gyrus as

Table 4. Between-group comparison of SPEM performance

Groups	Variables	0.2 Hz	0.4 Hz
LS vs. ROP	Gain (%)	$t_{(89)} = 2.01, P = .047, d = 0.44$	$t_{(89)} = 2.34, P = .021, d = 0.51$
	RMSE (°)	$t_{(89)} = -2.51, P = .014, d = -0.54$	$t_{(89)} = -1.32, P = .189, d = -0.29$
	Frequency of saccades (N/s)	$t_{(89)} = -1.68, P = .096, d = -0.36$	$t_{(89)} = -1.28, P = .203, d = -0.28$
LS vs. HNS	Gain (%)	$t_{(97)} = 0.39, P = .695, d = 0.08$	$t_{(97)} = 1.39, P = .166, d = 0.28$
	RMSE (°)	$t_{(97)} = -0.10, P = .921, d = -0.02$	$t_{(97)} = -0.60, P = .550, d = -0.12$
	Frequency of saccades (N/s)	$t_{(97)} = -0.97, P = .334, d = -0.20$	$t_{(97)} = -0.90, P = .368, d = -0.18$
LS vs. HPS	Gain (%)	$t_{(96)} = 0.21, P = .832, d = 0.04$	$t_{(96)} = 1.52, P = .132, d = 0.31$
	RMSE (°)	$t_{(96)} = 0.003, P = .997, d = 0.00$	$t_{(96)} = -1.06, P = .293, d = -0.22$
	Frequency of saccades (N/s)	$t_{(96)} = 0.20, P = .845, d = 0.04$	$t_{(96)} = -0.27, P = .784, d = -0.06$
HNS vs. ROP	Gain (%)	$t_{(74)} = 1.42, P = .159, d = 0.33$	$t_{(74)} = 0.83, P = .410, d = 0.19$
	RMSE (°)	$t_{(74)} = -2.34, P = .022, d = -0.54$	$t_{(74)} = -0.71, P = .481, d = -0.16$
	Frequency of saccades (N/s)	$t_{(74)} = -0.65, P = .518, d = -0.15$	$t_{(74)} = -0.36, P = 0.723, d = -0.08$
HPS vs. HNS	Gain (%)	$t_{(81)} = 0.15, P = .883, d = 0.03$	$t_{(81)} = -0.03, P = .973, d = -0.01$
	RMSE (°)	$t_{(81)} = -0.11, P = .910, d = -0.02$	$t_{(81)} = 0.37, P = .710, d = 0.08$
	Frequency of saccades (N/s)	$t_{(81)} = -1.05, P = .299, d = -0.23$	$t_{(81)} = -0.58, P = .565, d = -0.13$
HPS vs. ROP	Gain (%)	$t_{(73)} = 1.53, P = .131, d = 0.35$	$t_{(73)} = 0.84, P = .406, d = 0.19$
	RMSE (°)	$t_{(73)} = -2.50, P = .014, d = -0.58$	$t_{(73)} = -0.43, P = .665, d = -0.10$
	Frequency of saccades (N/s)	$t_{(73)} = -1.69, P = .095, d = -0.39$	$t_{(73)} = -0.94, P = .352, d = -0.22$

Notes: LS, low-schizotypy; HPS, high positive schizotypy; HNS, high negative schizotypy; ROP, recent onset psychosis; RMSE, root mean square error.

well as superior medial gyrus and ACC (Supplementary figure 4 and table 16). This indicates that higher probability of being categorized as ROP was associated with increased task-based functional connectivity from right FEF to these clusters. There was no significant effect in the reverse (i.e., positive) contrast.

Discussion

The aim of the present study was to directly compare individuals with high levels of schizotypy and patients with psychotic disorders regarding SPEM performance as well as brain function and connectivity. Using traditional BOLD and connectivity analyses, no group differences could be observed. However, using machine-learning, a model to distinguish patients from controls was delineated for the right FEF seed region.

Differences Between Controls and Patients

Based on behavioral SPEM data, LS and ROP participants could not be classified as distinct groups. However, univariate results revealed higher RMSE in ROP compared to LS, in agreement with previous evidence of reduced SPEM performance in psychosis.^{31,33} In contrast to previous investigations, univariate analyses of gain and saccadic frequency were not significant. The small difference in RMSE and the absence of differences in the two other performance measures are surprising considering that the SPEM deficit is a highly reliable marker of psychosis.^{31,33} Importantly, at the descriptive level, effects were in the expected direction with small to medium effect sizes, but not significant after Bonferroni-correction (see table 4).

In line with the behavioral results but in contrast to previous investigations^{36,41–44} no significant differences between ROP, HPS, HNS and LS groups could be determined at the neural level for the SPEM or Velocity contrasts. The same pattern emerged for the connectivity maps of all seed regions and contrasts. Of note, the task networks associated with the SPEM and Velocity contrasts showed substantial overlap with previous investigations, tightly replicating the neural network underlying SPEM^{36,75,84–90} and its modulation by target velocity^{36,75,87}. This highlights the validity of our task design and data analytic approach. Similarly, task-related connectivity maps showed substantial overlap with a recent investigation⁷⁵ studying pursuit-related functional connectivity in a healthy sample performing the same task employed in this study. However, in the current investigation, SPEM-related connectivity maps were even more widespread, especially from LGN, V1 and V5 seed regions, potentially related to greater statistical power stemming from a larger sample size.

Classification of functional connectivity maps was significant only before correction for multiple comparisons (achieving trend-level significance after correction) for the right FEF seed region. As the analyses did not survive correction for multiple comparison, results should be interpreted with great caution. The PPI seed region was located in right medial FEF. Classification was based on connectivity from there to subcortical (e.g., striatum and thalamus) and cortical structures encompassing early visual areas, cingulate gyrus, parietal cortex (e.g., precuneus, superior parietal cortex), frontal cortex (e.g., superior frontal gyrus and frontal-medial cortex), hippocampus and cerebellum. These areas partially overlap

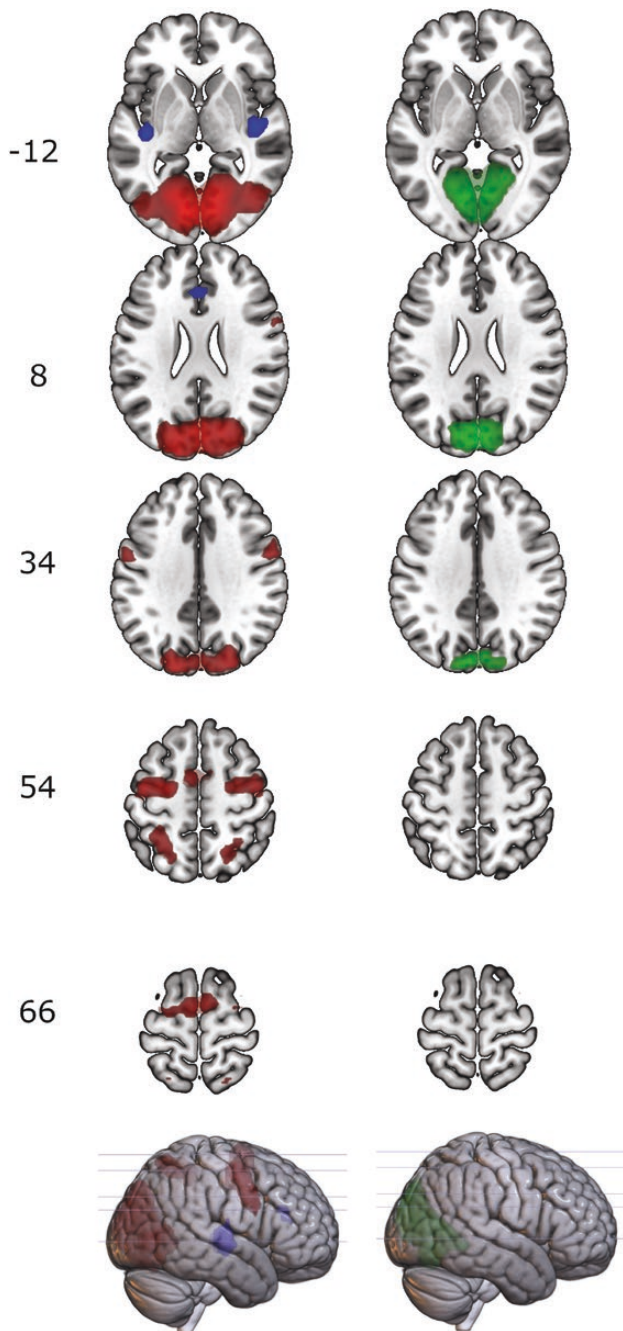


Fig. 2. Results of one-sample *t*-tests of the SPEM vs. fixation contrast (left, higher activation during SPEM is depicted in red, higher activation during fixation is depicted in blue) and high vs. low velocity contrasts (right, higher activation during high velocity SPEM is depicted in green, there was no higher activation during low velocity vs. high velocity SPEM), respectively ($n = 60$). Results are reported whole-brain family-wise error rate (FWE) corrected ($P < .001$, peak level) for clusters of at least 25 voxels. Labels on the left refer to the *z*-coordinate [Montreal Neurological Institute (MNI) space]. Slices were generated in MRICroGL.

with the known SPEM network but also include additional areas. For example, classification was based in part on connectivity from right FEF to hippocampus, which

is in line with previous reports that hyperactivity of that area during SPEM may be related to inhibitory dysfunction in schizophrenia.^{44,91}

Three explanations of the absence of group effects using traditional analyses and the rather subtle results combining functional connectivity and machine-learning approaches may be offered. First, the results could be explained by the diagnostic heterogeneity of the ROP group, given that the SPEM deficit is more pronounced in schizophrenia patients compared to patients with other disorders in the psychosis spectrum.³³ The inclusion of a variety of such spectrum disorders into our ROP group might have led to the rather subtle effects. However, the PANSS scores obtained here were similar to those of previous investigations that did find significant differences between patients and controls.^{67,91} All patients had ROP with average disorder duration of less than a year which could imply that SPEM deficits may not yet be fully developed. On the other hand, however, it has been demonstrated in a meta-analysis that duration of illness does not significantly influence SPEM dysfunction³¹.

A second possibility is insufficient power, which is why we conducted a post-hoc power analysis. According to this analysis, we had sufficient power to detect SPEM differences between controls and patients: Meta-analytical results from studies comparing SPEM performance of schizophrenia patients and controls show large effect sizes ($d = .70$ for RMSE, $d = .78$ for saccade frequency, and $d = .87$ for gain).³¹ With our sample size of $n = 62$ in the LS and $n = 34$ in the ROP group and an alpha-level of .05 we had a power of 0.94–0.99 to detect effect sizes in this range (*t*-tests, difference between two independent means). In addition, we used substantially larger samples than all previous BOLD fMRI investigations of SPEM in psychosis spectrum disorders^{36,41–44} suggesting that also at the neural level lack of power is not the main driver of the absence of group effects.

Third, it should be noted that behavioral performance in the LS group was lower than in other healthy control groups performing the same task in previous studies.^{36,92,93} It is therefore possible that the detection of significant group differences was impeded by the unusually poor performance in the control group. However, it has to be emphasized that control group participants were thoroughly screened and selected based on strict criteria to ensure suitability.

Schizotypy

Descriptively, at the behavioral level, both schizotypal samples showed intermediate SPEM performance levels between patients and control. This pattern of results was not significant, but reflects the expected direction of effects.^{35,37,38} At the neural level, in contrast to a previous study³⁶ traditional BOLD or functional connectivity analyses did not yield any evidence for group differences.

Table 5. Results of the machine-learning analyses for the gPPI contrasts

Seed region	Hemisphere	Con- trast	Sensitivity	Specificity	BAC	AUC	<i>P</i>	<i>P</i> _{corr}	
LGN	l	SPEM	63.6	36.4	49.8	0.51	.834	.834	
LGN	r		53.3	39.4	46.4	0.54	.633	.707	
V1	l		65.0	48.5	56.7	0.63	.184	.368	
V1	r		63.3	30.3	46.8	0.49	.636	.707	
V5+	l		78.3	27.3	52.8	0.58	.350	.583	
V5	r		85.0	27.3	56.1	0.52	.135	.338	
PPC+	l		81.7	36.4	59.0	0.61	.096	.338	
PPC	r		76.7	33.3	55.0	0.61	.135	.338	
FEF	l		63.3	48.5	55.9	0.56	.534	.707	
FEF+	r		73.3	51.5	62.4	0.63	.009	.090	
LGN	l		Velocity	51.7	48.5	50.1	0.47	.948	.949
LGN	r			46.7	45.5	46.1	0.46	.880	.949
V1	l			71.7	30.3	51.0	0.50	.897	.949
V1+	r			83.3	30.3	56.8	0.56	.117	.949
V5	l	81.7		21.2	51.4	0.50	.517	.949	
V5	r	78.3		24.2	51.3	0.44	.685	.949	
PPC	l	0		100.0	50.0	0.26	.653	.949	
PPC	r	50.0		48.5	49.2	0.45	.949	.949	
FEF	l	70.0		39.4	54.7	0.53	.462	.949	
FEF	r	11.7		69.7	40.7	0.43	.495	.949	

Notes: gPPI, generalized psychophysiological interaction analyses; LGN, lateral geniculate nucleus; PPC, posterior parietal cortex; FEF, frontal eye fields; BAC, balanced accuracy; AUC, area under the curve; P_{corr} , corrected *P*-value (false discovery rate correction⁸²).

*Permutation analyses with all 10 CV2 folds.

However, we also explored similarities and dissimilarities between psychosis and schizotypy by applying a machine-learning algorithm for SPEM seed regions trained on the LS and ROP groups to the schizotypal samples, thereby obtaining evidence of an involvement of right FEF. As the HPS and HNS groups did not differ from each other regarding SPEM performance, and the percentage of participants classified as ROP was virtually the same in both groups (HPS 39.0% vs HNS 39.1%), we treated them as one schizotypy group for subsequent analysis. Machine-learning decision scores for schizotypy groups were in between the LS and ROP groups and thus suggested that persons with high schizotypy could not be reliably classified as either LS or ROP. To identify brain areas that contributed to the assignment of HPS and HNS to ROP or LS, we explored how decision scores in the HPS and HNS samples were related to BOLD activity in those groups. Lower decision scores were associated with increased connectivity from right FEF to clusters in precuneus and angular gyrus, bilateral hippocampi, as well as postcentral and precentral gyrus. This pattern of results suggests that persons with high schizotypy may share some of the features underlying the pursuit deficits in ROP. Specifically, persons with high schizotypy may also show some degree of inhibitory dysfunction in hippocampus.^{44,91}

Conclusions

Overall, the present study constitutes a significant first step toward closing a crucial gap in the psychosis

literature, which is the lack of direct comparisons between individuals with high schizotypy and patients with psychosis. Critically, however, our data suggest that abnormalities of the pursuit response along the psychosis spectrum may be more subtle than previously reported. The data are partly in line with our initial suggestion that schizotypy is characterized by both similarities and dissimilarities with schizophrenia, which might explain why the SPEM deficit in schizotypy does not seem to be as consistent as may be expected from previous publications. Specifically, our results highlight that more emphasis should be placed on brain connectivity approaches which proved to be the most promising analyses for distinguishing groups along the psychosis spectrum. In summary, we strongly call for more large-scale, well-powered multi-center studies in order to gain a deeper understanding of SPEM-related deficits along the psychosis spectrum at both the behavioral and neural level.

Supplementary Material

Supplementary data are available at *Schizophrenia Bulletin Open* online.

Funding

This work was supported by Deutsche Forschungsgemeinschaft (ET 31/7-1; KO 3523/7-1; KA 4413/1-1). The PhD project of Rebekka Schröder is

funded by the German Academic Scholarship Foundation (Studienstiftung des deutschen Volkes). We acknowledge funding from the Open Access Publication Fund of the University of Bonn. The Authors have declared that there are no conflicts of interest in relation to the subject of this study.

Acknowledgments

We thank Johanna Gröning, Lena Hensel, Erik Lang, Melissa Reinelt, and Santiago Tovar for their help with data collection, and all volunteers for participating in the study.

References

- Ettinger U, Meyhöfer I, Steffens M, Wagner M, Koutsouleris N. Genetics, cognition, and neurobiology of schizotypal personality: a review of the overlap with schizophrenia. *Front Psychiatry*. 2014;5:18.
- Tonini E, Quidé Y, Kaur M, Whitford TJ, Green MJ. Structural and functional neural correlates of schizotypy: a systematic review. *Psychol Bull*. 2021;147(8)828–866.
- Nelson MT, Seal ML, Pantelis C, Phillips LJ. Evidence of a dimensional relationship between schizotypy and schizophrenia: a systematic review. *Neurosci Biobehav Rev*. 2013;37(3)317–327.
- Thomas EHX, Steffens M, Harms C, Rossell SL, Gurvich C, Ettinger U. Schizotypy, neuroticism, and saccadic eye movements: new data and meta-analysis. *Psychophysiology*. 2021;58(1)e13706.
- Steffens M, Meyhöfer I, Fassbender K, Ettinger U, Kambeitz J. Association of schizotypy with dimensions of cognitive control: a meta-analysis. *Schizophr Bull*. 2018;44(suppl_2):S512–S524.
- Liddle PF. The symptoms of chronic schizophrenia. *Br J Psychiatry*. 1987;151(2)145–151.
- Raine A, Reynolds C, Lencz T, Scerbo A, Triphon N, Kim D. Cognitive-perceptual, interpersonal, and disorganized features of schizotypal personality. *Schizophr Bull*. 1994;20(1)191–201.
- Schaefer J, Giangrande E, Weinberger DR, Dickinson D. The global cognitive impairment in schizophrenia: consistent over decades and around the world. *Schizophr Res*. 2013;150(1)42–50.
- Snitz BE. Cognitive deficits in unaffected first-degree relatives of schizophrenia patients: a meta-analytic review of putative endophenotypes. *Schizophr Bull*. 2005;32(1)179–194.
- Steen RG, Mull C, McClure R, Hamer RM, Lieberman JA. Brain volume in first-episode schizophrenia: systematic review and meta-analysis of magnetic resonance imaging studies. *Br J Psychiatry*. 2006;188:510–518.
- Hulshoff Pol HE, Kahn RS. What happens after the first episode? A review of progressive brain changes in chronically ill patients with schizophrenia. *Schizophr Bull*. 2007;34(2)354–366.
- Kühn S, Schubert F, Gallinat J. Higher prefrontal cortical thickness in high schizotypal personality trait. *J Psychiatr Res*. 2012;46(7)960–965.
- Shenton ME, Dickey CC, Frumin M, McCarley RW. A review of MRI findings in schizophrenia. *Schizophr Res*. 2001;49(1-2)1–52.
- Ettinger U, Williams SC, Meisenzahl EM, Möller H-J, Kumari V, Koutsouleris N. Association between brain structure and psychometric schizotypy in healthy individuals. *World J Biol Psychiatry*. 2012;13(7)544–549.
- Chapman LJ, Chapman JP, Kwapil TR, Eckblad M, Zinser MC. Putatively psychosis-prone subjects 10 years later. *J Abnorm Psychol*. 1994;103(2)171–183.
- van Os J, Linscott RJ, Myin-Germeys I, Delespaul P, Krabbendam L. A systematic review and meta-analysis of the psychosis continuum: evidence for a psychosis proneness–persistence–impairment model of psychotic disorder. *Psychol Med*. 2009;39(2)179–195.
- Giakoumaki SG. Cognitive and prepulse inhibition deficits in psychometrically high schizotypal subjects in the general population: relevance to schizophrenia research. *J Int Neuropsychol Soc*. 2012;18(4)643–656.
- Barrantes-Vidal N, Grant P, Kwapil TR. The role of schizotypy in the study of the etiology of schizophrenia spectrum disorders. *Schizophr Bull*. 2015;41(suppl 2)S408–S416.
- Ettinger U, Mohr C, Gooding DC, et al. Cognition and brain function in schizotypy: a selective review. *Schizophr Bull*. 2015;41(suppl 2)S417–S426.
- Debbane M, Eliez S, Badoud D, Conus P, Fluckiger R, Schultze-Lutter F. Developing psychosis and its risk states through the lens of schizotypy. *Schizophr Bull*. 2015;41(suppl 2)S396–S407.
- Mitelman SA, Shihabuddin L, Brickman AM, Hazlett EA, Buchsbaum MS. Volume of the cingulate and outcome in schizophrenia. *Schizophr Res*. 2005;72(2-3)91–108.
- Koo MS, Levitt JJ, Salisbury DF, Nakamura M, Shenton ME, McCarley RW. A cross-sectional and longitudinal magnetic resonance imaging study of orbitofrontal gyrus gray matter volume abnormalities in first-episode schizophrenia and first-episode affective psychosis. *Arch Gen Psychiatry*. 2008;74:6–760.
- Fornito A, Yücel M, Patti J, Wood SJ, Pantelis C. Mapping grey matter reductions in schizophrenia: an anatomical likelihood estimation analysis of voxel-based morphometry studies. *Schizophr Res*. 2009;108(1-3)104–113.
- Kasai K, Shenton ME, Salisbury DF, et al. Progressive decrease of left superior temporal gyrus gray matter volume in patients with first-episode schizophrenia. *Am J Psychiatry*. 2003;160(1)156–164.
- Zhou S-Y, Suzuki M, Takahashi T, et al. Parietal lobe volume deficits in schizophrenia spectrum disorders. *Schizophr Res*. 2007;89(1-3)35–48.
- Modinos G, Mechelli A, Ormel J, Groenewold NA, Aleman A, McGuire PK. Schizotypy and brain structure: a voxel-based morphometry study. *Psychol Med*. 2010;40(9)1423–1431.
- Nenadic I, Lorenz C, Langbein K, et al. Brain structural correlates of schizotypy and psychosis proneness in a non-clinical healthy volunteer sample. *Schizophr Res*. 2015;168(1–2)37–43.
- Batey M, Furnham A. The relationship between measures of creativity and schizotypy. *Personal Individ Differ*. 2008;45(8)816–821.
- Nelson B, Rawlings D. Relating schizotypy and personality to the phenomenology of creativity. *Schizophr Bull*. 2010;36(2)388–399.
- Hazlett EA, Goldstein KE, Kolaitis JC. A review of structural MRI and diffusion tensor imaging in schizotypal personality disorder. *Curr Psychiatry Rep*. 2012;14(1)70–78.
- O’Driscoll GA, Callahan BL. Smooth pursuit in schizophrenia: a meta-analytic review of research since 1993. *Brain Cogn*. 2008;68(3)359–370.

32. Levy DL, Sereno AB, Gooding DC, O'Driscoll GA. Eye tracking dysfunction in schizophrenia: characterization and pathophysiology. *Curr Top Behav Neurosci*. 2010;4:311–347.
33. Lencer R, Sprenger A, Reilly JL, et al. Pursuit eye movements as an intermediate phenotype across psychotic disorders: evidence from the B-SNIP study. *Schizophr Res*. 2015;169(0)326–333.
34. Koychev I, Joyce D, Barkus E, et al. Cognitive and oculomotor performance in subjects with low and high schizotypy: implications for translational drug development studies. *Transl Psychiatry*. 2016;6(5)e811–e811.
35. Lenzenweger MF, O'Driscoll GA. Smooth pursuit eye movement and schizotypy in the community. *J Abnorm Psychol*. 2006;115(4)779–786.
36. Meyhöfer I, Steffens M, Kasparbauer A-M, Grant P, Weber B, Ettinger U. Neural mechanisms of smooth pursuit eye movements in schizotypy. *Hum Brain Mapp*. 2015;36(1)340–353.
37. Smyrnis N, Evdokimidis I, Mantas A, et al. Smooth pursuit eye movements in 1,087 men: effects of schizotypy, anxiety, and depression. *Exp Brain Res*. 2007;179(3)397–408.
38. Holahan A-LV, O'Driscoll GA. Antisaccade and smooth pursuit performance in positive- and negative-symptom schizotypy. *Schizophr Res*. 2005;76(1)43–54.
39. Gooding DC, Miller MD, Kwapil TR. Smooth pursuit eye tracking and visual fixation in psychosis-prone individuals. *Psychiatry Res*. 2000;93(1)41–54.
40. Meyhöfer I, Steffens M, Faiola E, Kasparbauer A-M, Kumari V, Ettinger U. Combining two model systems of psychosis: the effects of schizotypy and sleep deprivation on oculomotor control and psychotomimetic states. *Psychophysiology*. 2017;54(11)1755–1769.
41. Hong LE, Tagamets M, Avila M, Wonodi I, Holcomb H, Thaker GK. Specific motion processing pathway deficit during eye tracking in schizophrenia: a performance-matched functional magnetic resonance imaging study. *Biol Psychiatry*. 2005;57(7)726–732.
42. Keedy SK, Ebens CL, Keshavan MS, Sweeney JA. Functional magnetic resonance imaging studies of eye movements in first episode schizophrenia: smooth pursuit, visually guided saccades and the oculomotor delayed response task. *Psychiatry Res*. 2006;146(3)199–211.
43. Lencer R, Nagel M, Sprenger A, Heide W, Binkofski F. Reduced neuronal activity in the V5 complex underlies smooth-pursuit deficit in schizophrenia: evidence from an fMRI study. *NeuroImage*. 2005;24(4)1256–1259.
44. Tregellas JR, Tanabe JL, Miller DE, Ross RG, Olincy A, Freedman R. Neurobiology of smooth pursuit eye movement deficits in schizophrenia: an fMRI study. *Am J Psychiatry*. 2004;161(2)315–321.
45. Krishna N, O'Neill H, Sanchez-Morla EM, Thaker GK. Long range frontal/posterior phase synchronization during remembered pursuit task is impaired in schizophrenia. *Schizophr Res*. 2014;157(1–3)198–203.
46. Boksman K, Théberge J, Williamson P, et al. A 4.0-T fMRI study of brain connectivity during word fluency in first-episode schizophrenia. *Schizophr Res*. 2005;75(2-3)247–263.
47. Fogelson N, Litvak V, Peled A, Fernandez-del-Olmo M, Friston KJ. The functional anatomy of schizophrenia: a dynamic causal modeling study of predictive coding. *Schizophr Res*. 2014;158(1–3)204–212.
48. Lynall M-E, Bassett DS, Kerwin R, et al. Functional connectivity and brain networks in schizophrenia. *J Neurosci*. 2010;30(28)9477–9487.
49. Wang Y-M, Cai X, Zhang R-T, et al. Altered brain structural and functional connectivity in schizotypy. *Psychol Med*. 2020;52(5):1–10. doi:10.1017/S0033291720002445.
50. Nelson MT, Seal ML, Phillips LJ, Merritt AH, Wilson R, Pantelis C. An investigation of the relationship between cortical connectivity and schizotypy in the general population. *J Nerv Ment Dis*. 2011;199(5)348–353.
51. P K, F S, A D, P A. High schizotypy traits are associated with reduced hippocampal resting state functional connectivity. *Psychiatry Res Neuroimaging*. 2021;307:111215.
52. Wang Y, Ettinger U, Meindl T, Chan RCK. Association of schizotypy with striatocortical functional connectivity and its asymmetry in healthy adults. *Hum Brain Mapp*. 2018;39(1)288–299.
53. Waltmann M, O'Daly O, Egerton A, et al. Multi-echo fMRI, resting-state connectivity, and high psychometric schizotypy. *Neuroimage Clin*. 2019;21:101603.
54. Wang Y, Yan C, Yin D, et al. Neurobiological changes of schizotypy: evidence from both volume-based morphometric analysis and resting-state functional connectivity. *SCHBUL*. 2015;41(Suppl 2)S444–S454.
55. Trajkovic J, Di Gregorio F, Ferri F, Marzi C, Diciotti S, Romei V. Resting state alpha oscillatory activity is a valid and reliable marker of schizotypy. *Sci Rep*. 2021;11(1)10379.
56. Davatzikos C. Why voxel-based morphometric analysis should be used with great caution when characterizing group differences. *NeuroImage*. 2004;23(1)17–20.
57. Fu CH, Mourao-Miranda J, Costafreda SG, et al. Pattern classification of sad facial processing: toward the development of neurobiological markers in depression. *Biol Psychiatry*. 2008;63(7)656–662.
58. Koutsouleris N, Meisenzahl EM, Davatzikos C, et al. Use of neuroanatomical pattern classification to identify subjects in at-risk mental states of psychosis and predict disease transition. *Arch Gen Psychiatry*. 2009;66(7)700–712.
59. Orrù G, Pettersson-Yeo W, Marquand AF, Sartori G, Mechelli A. Using support vector machine to identify imaging biomarkers of neurological and psychiatric disease: a critical review. *Neurosci Biobehav Rev*. 2012;36(4)1140–1152.
60. Koutsouleris N, Borgwardt S, Meisenzahl EM, Bottlender R, Möller H-J, Riecher-Rössler A. Disease prediction in the at-risk mental state for psychosis using neuroanatomical biomarkers: results from the FePsy study. *Schizophr Bull*. 2012;38(6)1234–1246.
61. Kaufmann T, Skåtun KC, Alnæs D, et al. Disintegration of sensorimotor brain networks in schizophrenia. *SCHBUL*. 2015;41(6)1326–1335.
62. Chyzyk D, Savio A, Graña M. Computer aided diagnosis of schizophrenia on resting state fMRI data by ensembles of ELM. *Neural Netw*. 2015;68(5)23–33.
63. Kambeitz J, Kambeitz-Illankovic L, Leucht S, et al. Detecting neuroimaging biomarkers for schizophrenia: a meta-analysis of multivariate pattern recognition studies. *Neuropsychopharmacology*. 2015;40(7)1742–1751.
64. Modinos G, Pettersson-Yeo W, Allen P, McGuire PK, Aleman A, Mechelli A. Multivariate pattern classification reveals differential brain activation during emotional processing in individuals with psychosis proneness. *NeuroImage*. 2012;59(3)3033–3041.
65. Madsen KH, Krohne LG, Cai X, Wang Y, Chan RCK. Perspectives on machine learning for

- classification of schizotypy using fMRI data. *Schizophr Bull.* 2018;44(suppl_2)S480–S490.
66. Lencer R, Trillenber P. Neurophysiology and neuroanatomy of smooth pursuit in humans. *Brain Cogn.* 2008;68(3)219–228.
 67. Nagel M, Sprenger A, Nitschke M, *et al.* Different extraretinal neuronal mechanisms of smooth pursuit eye movements in schizophrenia: An fMRI study. *NeuroImage.* 2007;34(1)300–309.
 68. Grant P, Kuepper Y, Mueller EA, Wielpuetz C, Mason O, Hennig J. Dopaminergic foundations of schizotypy as measured by the German version of the Oxford-Liverpool Inventory of Feelings and Experiences (O-LIFE)—a suitable endophenotype of schizophrenia. *Front Hum Neurosci.* 2013;7(1). doi:10.3389/fnhum.2013.00001.
 69. Miller TJ, McGlashan TH, Woods SW, *et al.* Symptom assessment in schizophrenic prodromal states. *Psychiatr Q.* 1999;70(4)273–287.
 70. Ackenheil M, Stotz-Ingenlath G, Dietz-Bauer R, Vossen A. MINI Mini International Neuropsychiatric Interview, German version 5.0.0 DSM IV. *Psychiatrische Universitätsklinik München, Germany.* 1999.
 71. Schultze-Lutter F, Addington J, Ruhrmann S, Klosterkötter J. *Schizophrenia Proneness Instrument, Adult Version (SPI-a).* Rome: Giovanni Fioriti Editore; 2007.
 72. Wechsler D. *Wais-III administration and scoring manual.* San Antonio, TX: The Psychological Association 1997.
 73. Friston KJ, Buechel C, Fink GR, Morris J, Rolls E, Dolan R. Psychophysiological and modulatory interactions in neuroimaging. *NeuroImage.* 1997;6(3)218–229.
 74. McLaren DG, Ries ML, Xu G, Johnson SC. A generalized form of context-dependent psychophysiological interactions (gPPI): a comparison to standard approaches. *NeuroImage.* 2012;61(4)1277–1286.
 75. Schröder R, Kasparbauer A-M, Meyhöfer I, Steffens M, Trautner P, Ettinger U. Functional connectivity during smooth pursuit eye movements. *J Neurophysiol.* 2020;124(6)1839–1856.
 76. Eickhoff SB, Stephan KE, Mohlberg H, *et al.* A new SPM toolbox for combining probabilistic cytoarchitectonic maps and functional imaging data. *NeuroImage.* 2005;25(4)1325–1335.
 77. Filzmoser P, Liebmann B, Varmuza K. Repeated double cross validation. *J Chemom.* 2009;23(4)160–171.
 78. Koutsouleris N, Meisenzahl EM, Borgwardt S, *et al.* Individualized differential diagnosis of schizophrenia and mood disorders using neuroanatomical biomarkers. *Brain.* 2015;138(7)2059–2073.
 79. Dukart J, Schroeter ML, Mueller K. Age correction in dementia—matching to a healthy brain. *PLoS One.* 2011;6(7)e22193.
 80. Kambeitz-Ilankovic L, Meisenzahl EM, Cabral C, *et al.* Prediction of outcome in the psychosis prodrome using neuroanatomical pattern classification. *Schizophr Res.* 2016;173(3)159–165.
 81. Xiao Y, Yan Z, Zhao Y, *et al.* Support vector machine-based classification of first episode drug-naïve schizophrenia patients and healthy controls using structural MRI. *Schizophr Res.* 2019;214(1)11–17.
 82. Benjamini Y, Hochberg Y. Controlling the false discovery rate: a practical and powerful approach to multiple testing. *J R Stat Soc Ser B (Methodological).* 1995;57(1)289–300.
 83. Gómez-Verdejo V, Parrado-Hernández E, Tohka J. Sign-consistency based variable importance for machine learning in brain imaging. *Neuroinformatics.* 2019;17(4)593–609.
 84. Dieterich M, Muller-Schunk S, Stephan T, Bense S, Seelos K, Yousry TA. Functional magnetic resonance imaging activations of cortical eye fields during saccades, smooth pursuit, and optokinetic nystagmus. *Ann N Y Acad Sci.* 2009;1164:282–292.
 85. Kimmig H, Ohlendorf S, Speck O, *et al.* fMRI evidence for sensorimotor transformations in human cortex during smooth pursuit eye movements. *Neuropsychologia.* 2008;46(8)2203–2213.
 86. Konen CS, Kleiser R, Seitz RJ, Bremmer F. An fMRI study of optokinetic nystagmus and smooth-pursuit eye movements in humans. *Exp Brain Res.* 2005;165(2)203–216.
 87. Nagel M, Sprenger A, Hohagen F, Binkofski F, Lencer R. Cortical mechanisms of retinal and extraretinal smooth pursuit eye movements to different target velocities. *NeuroImage.* 2008;41(2)483–492.
 88. Lencer R, Nagel M, Sprenger A, *et al.* Cortical mechanisms of smooth pursuit eye movements with target blanking. An fMRI study. *Eur J Neurosci.* 2004;19(5)1430–1436.
 89. Ohlendorf S, Sprenger A, Speck O, Glauche V, Haller S, Kimmig H. Visual motion, eye motion, and relative motion: a parametric fMRI study of functional specializations of smooth pursuit eye movement network areas. *J Vis.* 2010;10(14)21.
 90. Tanabe J, Tregellas J, Miller D, Ross RG, Freedman R. Brain activation during smooth-pursuit eye movements. *NeuroImage.* 2002;17(3)1315–1324.
 91. Tanabe J, Tregellas JR, Martin LF, Freedman R. Effects of nicotine on hippocampal and cingulate activity during smooth pursuit eye movement in schizophrenia. *Biol Psychiatry.* 2006;59(8)754–761.
 92. Steffens M, Becker B, Neumann C, *et al.* Effects of ketamine on brain function during smooth pursuit eye movements. *Hum Brain Mapp.* 2016;37(11)4047–4060.
 93. Kasparbauer A-M, Meyhöfer I, Steffens M, *et al.* Neural effects of methylphenidate and nicotine during smooth pursuit eye movements. *NeuroImage.* 2016;141:52–59.